

Preparing arrays of large atomically flat regions on single crystal substrates

F El Gabaly^{1,2}, N C Bartelt¹ and A K Schmid²

¹ Sandia National Laboratories, Livermore, CA 94550, USA

² Lawrence Berkeley National Laboratory, Berkeley, CA 94720, USA

E-mail: felgabaly@gmail.com

Received 26 December 2008

Published 7 July 2009

Online at stacks.iop.org/JPhysCM/21/314019

Abstract

We report a simple and general procedure to create arrays of atomically flat terraces on single crystal surfaces. Facets of three-dimensional (3D) metal islands formed after hetero-epitaxial growth are often flat and, through annealing or growth at elevated temperature, the formation of rather large (micron-scale) atomically flat-top facets can be promoted. We find that the step-free nature of top facets on such islands can be transferred to the substrate surface through room-temperature ion-sputter etching, followed by an annealing step. We use low-energy electron microscopy (LEEM) and Auger electron spectroscopy (AES) for *in situ* monitoring of the process steps while fabricating arrays of step-free surface regions on W(110), Ru(0001), Cu(100), and Fe(100) single crystals.

(Some figures in this article are in colour only in the electronic version)

1. Introduction

Atomic-height steps are a common feature of solid surfaces and they play important roles in many processes. Steps can have important catalytic [1, 2] and magnetic [3, 4] properties. Also, steps are often nucleation sites during epitaxial growth, so they can strongly affect the structure and properties of deposited films [5]. The practical importance of being able to control density and arrangement of surface steps through surface processing has long been recognized in the semiconductor industry, where wafers are often cut and polished at some controlled ‘miscut’ angle, a few degrees off with respect to the nominal orientation of the crystal lattice. The resulting surface step morphology is used as a parameter to optimize subsequent processing.

It is interesting to explore consequences of the *absence* of surface steps. In the absence of atomic surface steps, on essentially defect-free substrate regions, how would basic surface phenomena such as epitaxy or catalysis differ from more common situations involving stepped substrates? Understanding the properties of perfect, step-free surfaces and films grown on them is fundamentally interesting and may also enable novel nanotechnologies and device applications. Flat surfaces can form naturally during crystal growth because low-index surfaces are thermodynamically preferred [6]. However, conventional substrate preparations based on cutting and

polishing single crystals generally result in surfaces that contain a substantial density of steps, because finite process accuracy results in a finite miscut angle. (Even with good process control, it is difficult to reduce miscut below 0.1° , on average this corresponds to of the order of five atomic-height steps per micrometer.) Yet, even on conventionally prepared substrate crystals, step density often fluctuates across the surface and it is sometimes possible to find large step-free regions serendipitously. Figure 1 shows several examples of step-patterns we find on clean low-index metal surfaces, showing typical cases of relatively high step density, and one example of a localized flat surface region that is surrounded by a high step density area.

Growing epitaxial metal films on metal substrates in regions where substrate steps are absent can lead to qualitatively different structures than one would obtain on stepped substrates. For example, we recently showed that on step-free Ru(0001) terraces, layer-by-layer growth of Co films can be extended to substantially larger thickness than on stepped Ru(0001) surfaces, leading to the observation of previously unknown magnetic phenomena [7–9].

Such findings motivate the search for methods of preparing large step-free surface regions. Several groups have reported success in producing arrays of atomically flat regions on semiconductors [10–12] as well as on oxides [13] by patterning the substrates prior to final cleaning and annealing procedures.

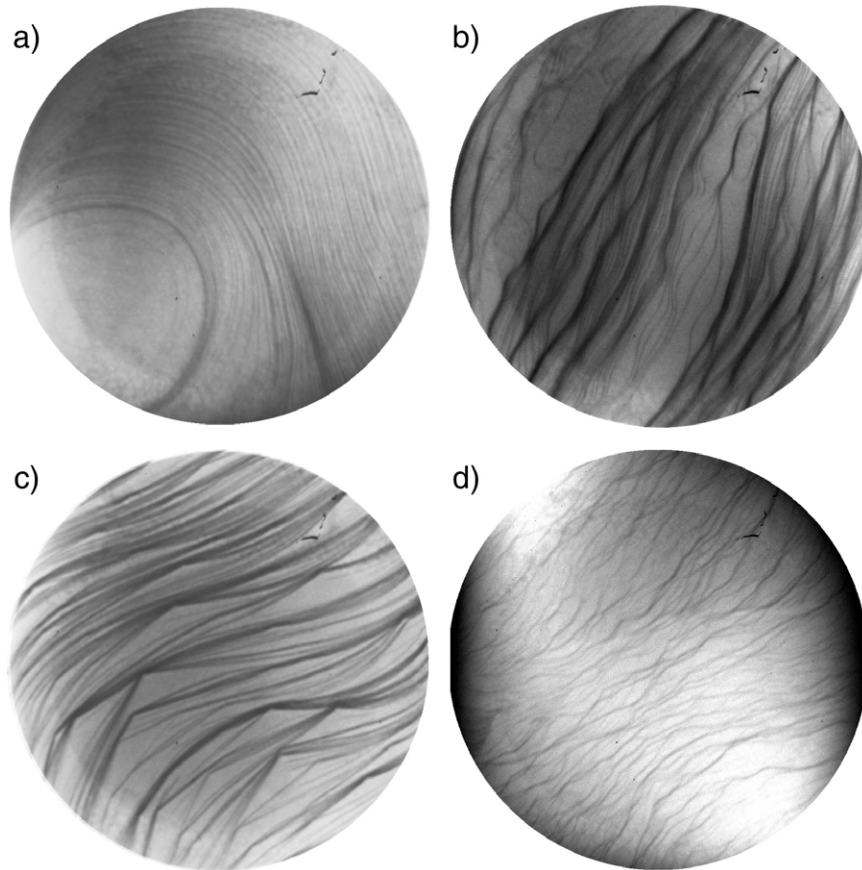


Figure 1. LEEM images (field of view $5\ \mu\text{m}$) of (a) W(110), (b) Ru(0001), (c) Cu(100), and (d) Fe(100) single crystal substrates. The thin lines are single atomic steps. The step densities observed in these images are typical for well-prepared low-index substrate surfaces. Note that in (a) a relatively large atomically flat region was found serendipitously. The atomically flat W(110) region is surrounded by regions with particularly high density of steps.

In these processes, lithographically produced trenches or mounds are used as efficient sinks for surface steps that become mobile during annealing. A key point in these methods is that they do not rely on the achievement of particularly low miscut angle. Instead, the key is to promote step bunching, so that the resulting surface is composed of alternating regions where step density is either particularly high (for example at the edges of mounds or trenches) or extremely low (further away from the edges).

The applicability of lithography is not universal, in part because lithography tools are often optimized to process semiconductor wafers, and are not necessarily suitable for less standardized shapes of crystal substrates used in research. Searching for a simple and generally applicable method to promote the formation of large, ultraflat surface regions, we recall that low-index surfaces are thermodynamically preferred [6]. Many epitaxial thin film systems are known where the film material grows in the form of small three-dimensional crystals, or islands. Following the Bauer-criterion [14], large differences of surface free energy between substrate and film material promote the formation of 3D islands, either in the Volmer–Weber or in the Stranski–Krastanov growth mode (with 3D islands formed directly on the substrate surface, or on top of a thin wetting layer, respectively). Very often, facets formed on these 3D islands are extremely flat.

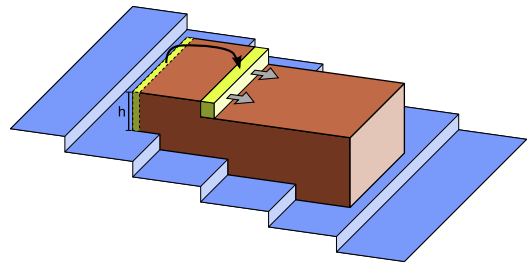


Figure 2. Schematic of a 3D hetero-epitaxial island during annealing, showing that the tendency of the island to dewet the substrate will move steps off the top of the island.

The reason for this flatness is that there is a strong driving force to remove steps from the top of the islands when they are much thinner than their equilibrium thickness. The source of this force is seen schematically in figure 2. If atoms are taken from an edge of an unstrained island of height h and attached to a step-edge on the upper surface, the energy change per moved atom is

$$\frac{1}{\rho h}(\gamma_{\text{substrate}} - \gamma_{\text{interface}} - \gamma_{\text{surface}})$$

where ρ is the atomic density of the island and $\gamma_{\text{substrate}}$, $\gamma_{\text{interface}}$, and γ_{surface} are the free energies per unit area of the island surface, the island-substrate interface, and the substrate

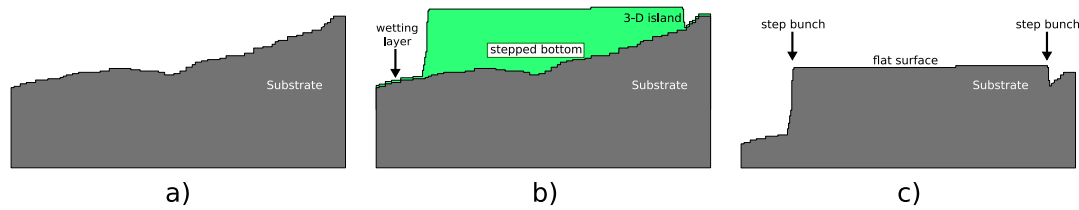


Figure 3. Cross-sectional schematic illustrating the flattening process. The vertical scale is exaggerated for clarity. (a) Low-index surface of a well-prepared single crystal, representing typical surfaces as shown in figure 1. (b) Growth of overlayer material in Stranski–Krastanov mode; the film material forms 3D islands on top of a thin wetting layer. The top facets of the islands have formed step-free low-index surfaces. (c) After a uniform sputter-etching of the surface, all the overlayer material and part of the substrate material is removed. As a result, the shapes of the overlayer islands were transferred into the substrate surface.

(possibly wetting layer covered) surface, respectively. Thus when $\gamma_{\text{substrate}} - \gamma_{\text{interface}} - \gamma_{\text{surface}} < 0$ —the Bauer criterion [14] for the formation of 3D islands—steps will be driven to the island edge, with a force that becomes larger as h becomes smaller. In principle the island could decrease its free energy even more by adding new layers and growing thicker, but the barrier for new layer nucleation often prevents this [15–17]. This effective height constraint causes these ‘mesas’ to have much larger top step-free facets than even shape-equilibrated islands [16, 18]. Thus, large step-free facets are often observed features of annealed dewetting films [15, 19].

In the context of surface science research, such facets on the surface of freshly grown 3D islands can sometimes be used as high-quality, step-free substrates. For example, we previously used the top facets of Cu islands on a Ru(0001) surface as Cu(111) substrates with excellent quality [20].

The growth of flat-topped 3D islands can be a simple and appealing way to fabricate large step-free surface regions. Useful guides to help identify candidate materials for growing 3D islanded films include literature summarizing surface free energy values [21, 22] and discussions of intermetallic phase formation [23, 24], since alloying would tend to interfere with the aims we pursue here (obtain flat, clean substrates).

2. Step-free surface preparation on a wide range of substrates

Not all materials are easily deposited or form large flat-topped islands during growth, however, motivating the central point of this paper: we report a simple step-by-step process, based on growth of flat-topped islands first, that can be used to drastically expand the range of materials and surface orientations that can be processed into extended arrays of step-free surface regions. The idea is that the morphology of flat-topped 3D islands can be transferred into the underlying substrate surface by a gentle ion-sputter-etching process. This procedure of creating arrays of large step-free regions on a chosen substrate with high step density is summarized in figure 3: (i) Grow and anneal flat-topped 3D epitaxial islands of a suitable overlayer material on the chosen substrate. This can be achieved by selecting an overlayer material that grows in Stranski–Krastanov (wetting layer + 3D islands) or Volmer–Weber (3D island) mode. (ii) Completely remove the islanded film again by ion-sputter etching. Sputtering

conditions (i.e. energy, ion type) are chosen so that sputter rates of the overlayer material and substrate material are similar—under such conditions, substrate regions that were outside of the footprints of 3D islands are etched continuously, while the etching of substrate regions that are hidden under the footprints of 3D islands is delayed until the islands themselves have been etched away. As a result, after sputtering, the cleaned substrate surface has a topography composed of flat-topped mounds separated by trenches, mirroring the previous array of flat-topped islands. (iii) Annealing to heal surface defects induced by the sputtering.

Because of the common tendency of thin films to form flat 3D islands on closepacked metal surfaces, we believe that applicability of our method is general. In the following paragraphs, we show how step-free regions were prepared on W(110) (using Co as overlayer material), Ru(0001) (using Co as overlayer material), Cu(100) (using bi-layers of Ag and Co as patterning films), and Fe(100) (using Bi as overlayer material). We indicate process parameters in some detail, although we would like to point out that further optimization is very likely possible. The method appears to be robust and results based on process parameters given here are reproducible. In addition, we also expect that variation of process parameters (or film/substrate material choices) will permit fabrication of a variety of different types of arrays of ultraflat surface regions.

Refractory metals such as tungsten and ruthenium have substantially higher surface free energy than transition metals. Therefore, according to Bauer’s criterion [14], deposition of transition metals on refractory metal substrates leads to the formation of 3D islands in a Stranski–Krastanov growth mode. Although we expect that a variety of overlayer materials will produce similar results, we found it convenient to use Co films for processing W(110) and Ru(0001) substrates. In ultra-high vacuum conditions (the background pressure remained below 10^{-10} Torr throughout all our film depositions) we first deposited 10 ML of Co at a growth rate of 1.9 ML min^{-1} , while substrate temperatures were held at 100°C for the W(110) crystal and 250°C for the Ru(0001) substrate. After the first ten layers the temperature of the substrates was increased to 600°C and the Co deposition rate was increased to 3 ML min^{-1} . At this point, 3D islands started to form, with atomically flat-top facets. Figure 4 shows the Co islands on a W(110) substrate. They grew in lateral size until they

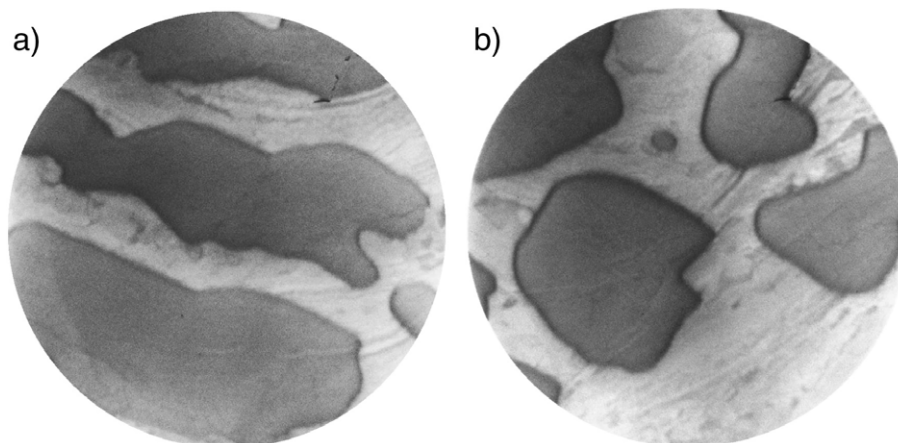


Figure 4. LEEM images (field of view $5\ \mu\text{m}$) of 60 ML thick islands (dark gray) of Co on W(110). Between the islands, the surface is covered with 2 ML of Co (wetting layer). (a) and (b) shows two different regions of the surface.

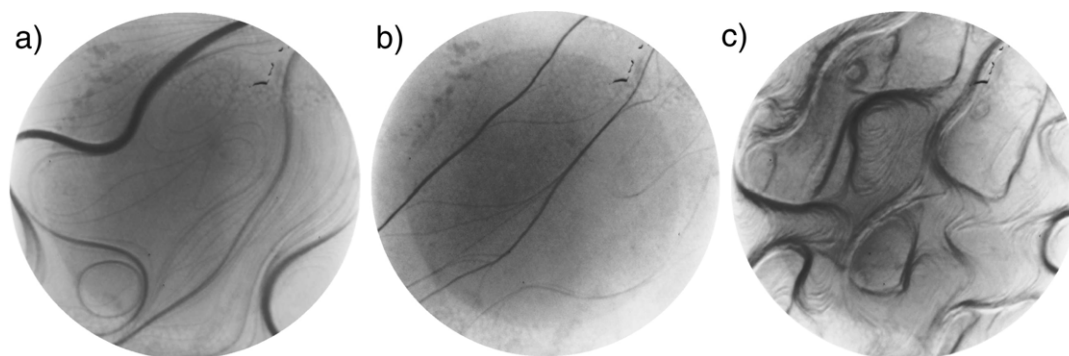


Figure 5. LEEM images (field of view $5\ \mu\text{m}$) of clean W(110) (a), Ru(0001) (b), and Cu(100) (c) surfaces after completion of the processing described in this paper.

covered 50% of the surface, while the remaining surface area was covered by two atomic layers of Co (wetting layer). After depositing a total dose equivalent to 30 continuous atomic layers of cobalt, the deposition was stopped and the sample was allowed to cool down. The entire process was monitored *in situ* by LEEM (our instrument is described in more detail in [25]). The substrate was then transferred within the chamber to a position where the sample faced a sputter ion-source. With sample temperature near 30°C , the surface was sputter etched for 1 h, using 2000 eV Ar ions at an ion-current density of, very approximately, $\sim 5\ \mu\text{A cm}^{-2}$. The result was the homogeneous removal of all the Co and part of the substrate material. *In situ* Auger electron spectroscopy (AES) was used to confirm that all Co had been removed. (We should note that in the range of systems we have explored so far, we find that the quality of results does not depend very sensitively on the sputtering parameters, as long as complete removal of the film is achieved.) Finally, the samples were treated with three cycles of flash annealing in a 3×10^{-8} Torr oxygen atmosphere, followed by two flash-annealing cycles in ultra-high vacuum (UHV) to remove oxygen from the surfaces (we anneal W to 2000°C and Ru to 1700°C).

Inspection by LEEM confirms that the flat-top island morphology of the cobalt film was successfully transferred into

the pure tungsten and ruthenium substrates. LEEM images reproduced in figure 5(a)–(b) show that in both cases the substrates now have large atomically flat, step-free, regions on their surfaces.

The usefulness of the Stranski–Krastanov growth mode to fabricate 3D islands can be extended beyond refractory substrates by choosing overlayer materials with particularly low surface free energy. For example, to work with the transition metal substrate Fe(100), we chose to deposit films of bismuth. Soon after the beginning of the Bi deposition on clean, stepped Fe(100) at 300°C substrate temperature, a large number of islands appear uniformly distributed on the surface. The melting point of Bi is 271°C and these islands are in fact liquid drops. The drops grow in size as more material is being deposited, and they coalesce with neighboring drops when they get close enough. When the average drop size reached approximately $1\ \mu\text{m}$ diameter (figure 6(a)) we stopped the deposition and cooled the substrate to room temperature. Observing the LEEM image during cooling, solidification of the Bi drops is very clearly visible: the smooth contrast variation across the surface of liquid Bi drops abruptly and changes to a much sharper contrast variation, revealing the appearance of a large, flat facet on the tops of the solidified islands. These solid islanded Bi films were then removed by

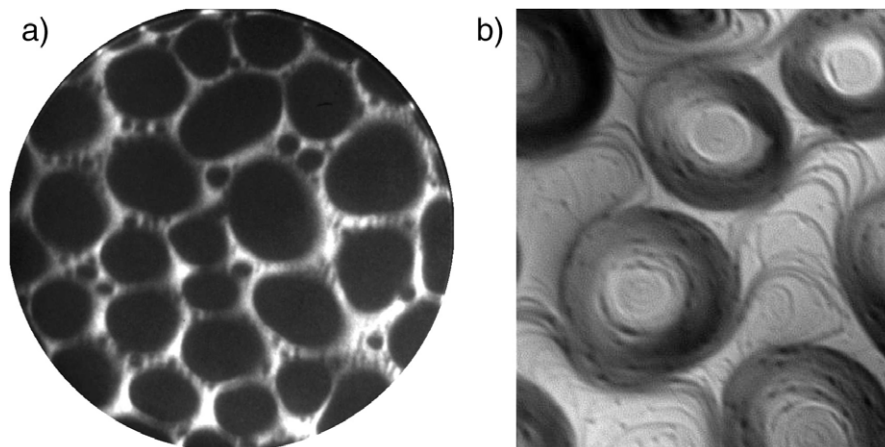


Figure 6. (a) Liquid Bi islands (black) on an Fe(100) surface (field of view $5\ \mu\text{m}$). (b) Clean Fe(100) surface after quenching the Bi, removing the Bi by sputter-etching, and annealing the clean Fe(100). The shapes of the Bi islands have been transferred into the Fe(100) surface. (Size: $2.6\ \mu\text{m} \times 3\ \mu\text{m}$.)

sputtering (150 min at $\sim 5\ \mu\text{A cm}^{-2}$ flux of 2000 eV Ar ions). After confirming complete removal of the Bi film, the Fe(100) crystal was annealed for 5 min at 425°C . Figure 6(b) shows the resulting array of step bunches that separate large, almost step-free areas. As expected, the surface topography clearly resembles the prior topography of the islanded Bi film.

Cu(100) is an interesting example because it illustrates how small process modifications can permit a dramatic expansion of the range of materials that can be processed with the same general approach. When we began to explore optimization of process parameters for fabricating step-free Cu(100) terraces, Co and Ag evaporators were already mounted on our LEEM system. Differences in the values of the surface free energy of the Cu substrate, compared to Co or Ag, are much smaller than in the case of the examples described above. Therefore, one might expect that the deposition of Co or Ag on Cu(100) would not easily form 3D islands. Indeed, in initial *in situ* growth experiments using Ag or Co, we were unable to fabricate large, flat-topped 3D islands on the Cu(100) surface. Recalling that Co/Cu(100) is a well-known epitaxial system that permits the growth of high-quality *uniform-thickness* films, and recalling that the surface free energy difference between Ag and Co is nearly twice as large as the difference between Cu and either overlayer material, we decided to use continuous, flat, Co/Cu(100) films as a buffer layer for the growth of Ag films. With the small modification of inserting a Co buffer layer, we found that Ag deposition allowed the fabrication of large flat-topped 3D islands and subsequent transfer of the pattern into the pure Cu(100) substrate.

In a specific preparation, we deposited 26 ML of Co at 150°C and a deposition rate of $1\ \text{ML min}^{-1}$ to form a uniform epitaxial film. Next, we deposited the equivalent of 40 ML of Ag on top of the 26 ML of Co, at a rate of $1.2\ \text{ML min}^{-1}$ and substrate temperature 300°C . The Ag film grew in a typical Stranski–Krastanov mode, forming flat-topped islands with an average diameter of the order of 500 nm. Oswald ripening induced by additional annealing at 450°C for 73 min increased the average island size, as shown in the time series reproduced

in figures 7(a)–(d). Sputtering at room temperature (80 min at $\sim 5\ \mu\text{A cm}^{-2}$ flux of 2000 eV Ar ions) completely removed the Ag islands and the Co buffer layer. A final flash-annealing step (maximum temperature 600°C for a few seconds) led to the array of large, ultraflat surface regions seen in the LEEM image in figure 5(c).

3. Discussion and outlook

Facets that form on the surfaces of 3D islands during their growth and annealing are often extremely flat, even when the islands are grown on top of substrates with a high density of steps. Underneath islands with step-free top facets, substrate surface steps can thus be buried and confined to a stepped substrate/island interface. We have demonstrated how, for a range of substrate/overlayer materials, ion-sputtering and annealing steps can be used to remove such 3D islands from surfaces, while transferring the flat-top topography of the islands into substrate surfaces. As a result of such processing, substrate crystal surfaces having some average density of surface steps (corresponding to miscut angle) are patterned to form arrays of micron-scale regions that are essentially free of surface steps, separated by step bunches.

More generally, we expect that the treatments that we describe in this paper can be adapted in order to fabricate arrays of ultraflat terraces on a wide variety of substrate crystals. The only requirement is that the substrate can be covered with a film that (i) forms flat-topped 3D islands and (ii) the film can be removed again by an ion-sputtering schedule that etches the substrate and film materials at similar rates. On many substrate materials, the growth of 3D overlayer islands can be promoted by depositing films of materials with appropriate values of their surface free energy [14, 21, 22]. Moreover, if no suitable overlayer material is available, an appropriate buffer layer can be grown on the substrate first, to optimize islanding in a subsequently deposited overlayer. Low selectivity of the ion etching process can be promoted by adjusting ion mass and energy, although for the material combinations that we used in this work, we found that details of the sputtering conditions

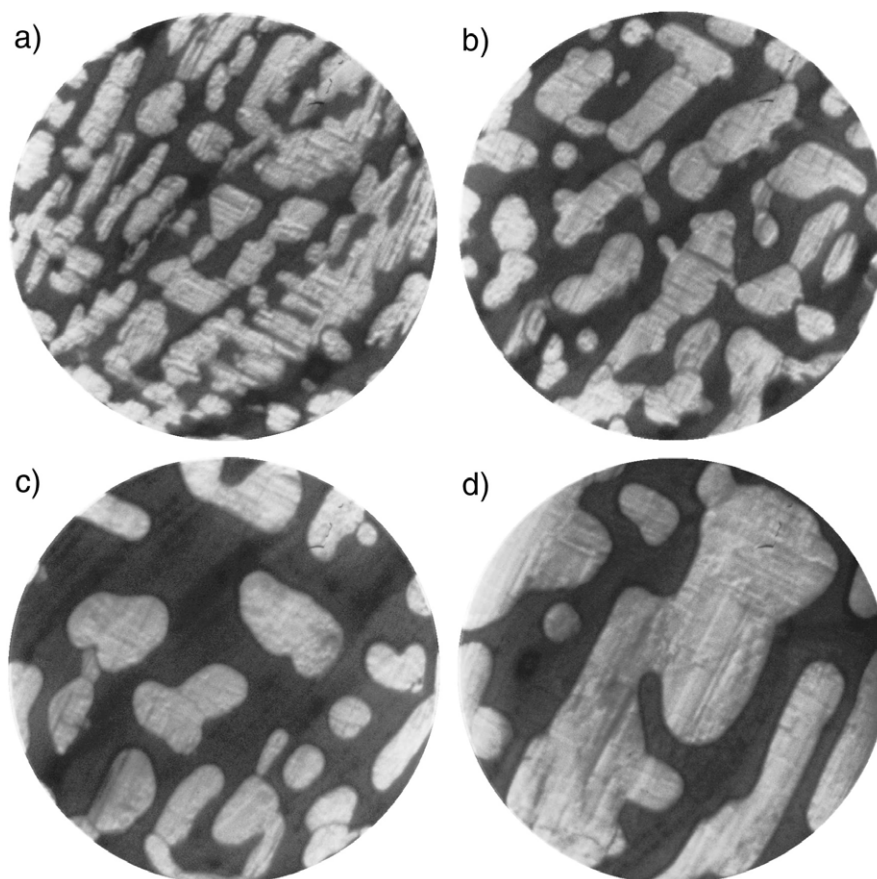


Figure 7. Time sequence of LEEM images of 50 ML thick islands of Ag on top of a continuous 26 ML thick film of Co (white) on Cu(100). The sequence shows how, during annealing at 450 °C, lateral size of the islands increases by Oswald ripening: (a) initial film (see text), (b) 17 min (c) 40 min, and (d) 73 min annealing time. The top facets of all the islands remain flat at all times. Line-patterns seen in the images of islands correspond to the step structure at the Ag/Co interface. Panel (c) of figure 5 shows the surface after the sputter-etching and annealing processes, when the island shapes have been transferred into the clean Fe(100) surface.

are not very important. The formation of overlayer islands with a desired large size commonly involves growth at elevated substrate temperature or annealing. Thus, the need to remove the film again implies that interdiffusion can be suppressed. Either kinetics or energetics can be taken into account in selecting film/substrate combinations that will not alloy. In cases where a tendency towards alloying might pose problems, one can also consider the use of a diffusion barrier, similar to the Co buffer layer we used while preparing flat regions on a Cu(100) crystal. As a result of the described procedures, large step-free regions can be formed on surfaces of many different types of substrates.

Acknowledgment

This research was supported by the US Department of Energy under contracts No. DE-AC02-05CH11231 and DE-AC04-94AL85000.

References

- [1] Somorjai G 1981 *Chemistry in Two Dimensions: Surfaces* (Ithaca, NY: Cornell University Press)
- [2] Davis S and Somorjai G 1982 *The Chemical Physics of Solid Surfaces and Heterogeneous Catalysis (Fundamental Studies of Heterogeneous Catalysis vol 4)* ed D King and D Woodruff (Amsterdam: Elsevier)
- [3] Rusponi S, Cren T, Weiss N, Epple M, Bulushech P, Claude L and Brune H 2003 *Nat. Mater.* **2** 546–51
- [4] Klein C, Ramchal R, Schmid A K and Farle M 2007 *Phys. Rev. B* **75** 193405
- [5] Brune H 1998 *Surf. Sci. Rep.* **31** 121–229
- [6] Conrad E H 1992 *Prog. Surf. Sci.* **39** 65
- [7] El Gabaly F, Gallego S, Muñoz C, Szunyogh L, Weinberger P, Klein C, Schmid A K, McCarty K F and de la Figuera J 2006 *Phys. Rev. Lett.* **96** 147202
- [8] El Gabaly F, Puerta J M, Klein C, Saa A, Schmid A K, McCarty K F, Cerda J I and de la Figuera J 2007 *New J. Phys.* **9** 80
- [9] El Gabaly F, McCarty K F, Schmid A K, de la Figuera J, Muñoz C, Szunyogh L, Weinberger P and Gallego S 2008 *New J. Phys.* **10** 73024
- [10] Tanaka S, Umbach C C, Blakely J M, Tromp R M and Mankos M 1996 *Appl. Phys. Lett.* **69** 1235
- [11] Homma Y, Hibino H, Ogino T and Aizawa N 1997 *Phys. Rev. B* **55** R10237
- [12] Lee D and Blakely J M 2000 *Surf. Sci.* **445** 32
- [13] Chang K C and Blakely J M 2003 *Mater. Res. Soc. Symp. Proc.* **749** 271
- [14] Bauer E 1958 *Z. Kristallogr.* **110** 372
- [15] Ling W L, Giessel T, Thürmer K, Hwang R Q, Bartelt N C and McCarty K F 2004 *Surf. Sci.* **570** L297
- [16] Mullins W W and Rohrer G S 2000 *J. Am. Ceram. Soc.* **83** 214
- [17] Thürmer K and Bartelt N C 2008 *Phys. Rev. Lett.* **100** 186101

-
- [18] Thürmer K, Reutt-Robey J E and Williams E D 2003 *Surf. Sci.* **537** 123
- [19] McCarty K F 2006 *Nano Lett.* **6** 858
- [20] Schmid A K, Bartelt N C and Hwang R Q 2000 *Science* **290** 1561
- [21] Vitos L, Ruban A V, Skriver H L and Kollar J 1998 *Surf. Sci.* **411** 186–202
- [22] Mezey L Z and Giber J 1982 *Japan. J. Appl. Phys.* **21** 1569–71
- [23] Hansen M and Anderko K 1958 *Constitution of Binary Alloys* (New York: McGraw-Hill)
- [24] Massalski T B 1987 *Binary Phase Diagrams* (Metals Park, OH: American Society for Metals)
- [25] Grzelakowski K and Bauer E 1996 *Rev. Sci. Instrum.* **67** 742